Dynamic subgrid-scale modeling of compressible turbulence

By Kyle D. Squires[1]

The dynamic subgrid-scale modeling concept formulated by Germano *et al.* (1991) for incompressible flows has been successfully extended to compressible turbulence. Most of the results of this extension have been reported by Moin *et al.* (1991). This report will serve to highlight the main accomplishments and unresolved issues and provide possible directions for future work and improvements to the concept of dynamic modeling for large-eddy simulation.

1. Motivation and objectives

The accurate prediction of turbulent flows at high Reynolds numbers remains a formidable challenge for computational fluid dynamics. Because of the rapid increase in the range of length scales with increasing Reynolds number, direct numerical simulation (DNS) is not feasible for predictions of high-Reynolds number turbulent flows of engineering interest. Thus, predictions of turbulence at high Reynolds numbers can only be obtained by solving some suitably averaged form of the Navier-Stokes equations. Averaging the governing equations gives rise to correlations of turbulence quantities which must be modeled using various levels of approximation. This report is concerned with subgrid-scale modeling for large-eddy simulation (LES).

To date, the accuracy of predictions of turbulent flows obtained using LES have been limited because of unreliable subgrid-scale models. The principal deficiency associated with previous subgrid modeling efforts has been an inability to predict a wide class of flows with a fixed set of model constants. This deficiency arises primarily because of the fact that nearly all previous models (subgrid or otherwise) have required *ad hoc* prescriptions of the model constants. The model constants used in these computations are usually calibrated to yield good agreement with a particular laboratory experiment or DNS computation. It is not surprising, therefore, that it is difficult to obtain accurate predictions of different flow fields in arbitrary geometries using the same model constants.

Many of the deficiencies associated with previous subgrid-scale modeling efforts were remedied by the recent work of Germano *et al.* (1991). Briefly, these investigators recognized that because the large-scale field in LES is computed *directly*, a great deal of information regarding the structural interactions of the resolved scales is available as part of the computation. The advance gained by Germano *et al.* was utilization of this information in formulation of the subgrid-scale model. Using an algebraic identity developed by Germano (1990), they formulated an eddy

1 Present address: The University of Vermont, Dept. of Mechanical Engineering

viscosity model for the subgrid scale stresses in which an expression for the model coefficient is obtained as a function of the local properties of the flow. To determine the model coefficient in this manner, it is first necessary to define the velocity field at two levels of resolution. It is further necessary to assume that the turbulent stresses at both levels of resolution are similar and may, therefore, be modeled using the same functional expression. Computations of transitional and fully-developed turbulent channel flows using this concept showed very good agreement with DNS data. It should be emphasized that in these computations, no *ad hoc* calibration of the model coefficient was required. The results obtained by Germano *et al.* were as good or better than previous LES computations in which "tuning" of the model constant was used to improve comparison of LES results and experimental data.

Given the encouraging results obtained by Germano *et al.* for incompressible turbulence, the primary objective of the present study was the extension of the dynamic modeling concept to compressible turbulence. The secondary objective of the work was *a posteriori* tests of the dynamic model using LES of homogeneous turbulence. In the first computation, LES of decaying, incompressible, isotropic turbulence was performed. The LES results were compared to the experimental data of Comte-Bellot & Corrsin (1971) (CBC hereafter). In the second computation, LES of decaying compressible, isotropic, turbulence was performed. For this case, LES results were compared to filtered DNS data. As is shown in Section 2, comparison of LES results to both laboratory experimental data and DNS data is excellent.

2. Accomplishments

In the first phase of the research, the dynamic modeling concept was extended to compressible turbulence. Only the salient features relevant to compressible turbulence are summarized in section 2.1. The reader is referred to Moin *et al.* (1991) for a complete derivation and discussion of the governing equations. Contained in section 2.2 are representative comparisons of LES results to the experimental data of CBC for incompressible turbulence. The reader is again referred to Moin *et al.* for a complete comparison of LES and experimental results for the simulations of incompressible turbulence. Comparison of LES results from simulations of compressible, isotropic turbulence to filtered DNS data are contained in section 2.3.

2.1 Model development

As shown in Moin *et al.* (1991), filtering the compressible Navier-Stokes equations yields the subgrid-scale stress, τ_{ij}, and subgrid-scale heat flux, q_j:

$$\tau_{ij} = \overline{\rho u_i u_j} - \frac{\overline{\rho u_i}\,\overline{\rho u_j}}{\overline{\rho}}, \tag{2.1a}$$

and

$$q_j = \overline{\rho u_j T} - \frac{\overline{\rho u_j}\,\overline{\rho T}}{\overline{\rho}}. \tag{2.1b}$$

In (2.1), u_i is the component of velocity in the i^{th} direction, and ρ and T are the fluid density and temperature, respectively. Throughout this work a filtered quantity is

denoted with an overbar. For compressible turbulence, it is also convenient to define a density-weighted (i.e., Favre-filtered) quantity as

$$\widetilde{f} = \frac{\overline{\rho f}}{\overline{\rho}}. \tag{2.2}$$

It is important to note that there are subgrid-scale quantities in addition to those given by (2.1) which arise upon filtering the compressible momentum and energy equations. For example, the viscous terms in the momentum equation as well as the viscous dissipation, pressure dilatation, and heat conduction terms in the thermal energy equation all have contributions at the subgrid-scale level. However, the objectives of the present study were the extension and testing of the dynamic modeling concept for compressible turbulence. Therefore, the neglect of these terms is justified in the present context.

The key element of the dynamic model concept is the utilization of spectral information contained in the resolved field in formulation of the subgrid-scale stress model. To incorporate spectral information into the model for the subgrid-scale stress, it is necessary to define an additional filter, known as the "test filter". The test filter applied to a function $\overline{f}$ is denoted as $\widehat{\overline{f}}$. Application of the test filter to the momentum equations yields the test-field stress, $\mathcal{T}_{ij}$. For compressible turbulence, this quantity is given by

$$\mathcal{T}_{ij} = \widehat{\overline{\rho u_i u_j}} - \frac{\widehat{\overline{\rho u_i}}\,\widehat{\overline{\rho u_j}}}{\widehat{\overline{\rho}}}. \tag{2.3}$$

As shown by Germano (1990), the test-field stress, $\mathcal{T}_{ij}$, and subgrid-scale stress, τ_{ij}, are related to the resolved turbulent stress, $\mathcal{L}_{ij}$:

$$\mathcal{L}_{ij} = \mathcal{T}_{ij} - \widehat{\tau}_{ij} = \widehat{\left(\frac{\overline{\rho u_i}\,\overline{\rho u_j}}{\overline{\rho}}\right)} - \frac{\widehat{\overline{\rho u_i}}\,\widehat{\overline{\rho u_j}}}{\widehat{\overline{\rho}}}. \tag{2.4}$$

The right-hand side of (2.4) may be explicitly evaluated as part of the computation. Therefore, manipulation of (2.4) will permit an expression to be obtained for τ_{ij} in terms of local flow properties. In the present study, the anisotropic part of τ_{ij} was modeled using the Smagorinsky (1963) eddy viscosity model:

$$\tau_{ij} - \frac{1}{3}q^2\delta_{ij} = -2C_S\overline{\rho}\Delta^2|\widetilde{S}|\left(\widetilde{S}_{ij} - \frac{1}{3}\widetilde{S}_{kk}\delta_{ij}\right), \tag{2.5}$$

where

$$\widetilde{S}_{ij} = \frac{1}{2}\left(\frac{\partial\widetilde{u}_i}{\partial x_j} + \frac{\partial\widetilde{u}_j}{\partial x_i}\right) \tag{2.6}$$

is the resolved-scale strain rate,

$$|\widetilde{S}| = \left(2\widetilde{S}_{ij}\widetilde{S}_{ij}\right)^{1/2} \tag{2.7}$$

is the magnitude of the strain-rate tensor, and q^2 is the isotropic part of τ_{ij}. The filter width associated with the grid level filter is denoted Δ in (2.5). In incompressible turbulence, q^2 may be absorbed into the pressure variable. However, the pressure in compressible turbulence satisfies its own evolution equation, and, therefore, the subgrid-scale energy must be explicitly modeled. As reported in Moin *et al.* (1991), the subgrid-scale energy is modeled using Yoshizawa's (1986) parameterization:

$$q^2 = 2C_I\overline{\rho}\Delta^2|\widetilde{S}|^2 . \tag{2.8}$$

The reader is referred to section 2.3 for further discussion of modeling the subgrid-scale energy.

As shown above, (2.5) and (2.8) are the models for the turbulent stresses at the grid level. If it is assumed that expressions similar to (2.5) and (2.8) may be used to parameterize the turbulent stresses at the test field level and further assumed that the model coefficients are identical at the grid and test field levels, then (2.4) may be used to obtain expressions for C_S and C_I in terms of local flow properties. For example, if the Smagorinsky model is used for the anisotropic part of τ_{ij} and $\mathcal{T}_{ij}$, then (2.4) may be written as

$$\mathcal{L}^*_{ij} = 2C_S M^*_{ij}, \tag{2.9}$$

where

$$M^*_{ij} = -\widehat{\overline{\rho}}\widehat{\Delta}^2|\widehat{\widetilde{S}}|\widehat{\widetilde{S}}^*_{ij} + \widehat{\overline{\rho}\Delta^2|\widetilde{S}|\widetilde{S}^*_{ij}} . \tag{2.10}$$

The * superscript on the tensors in (2.9), (2.10) and elsewhere in this manuscript denote the trace-free part of the tensor. An additional approximation has been made in (2.9) with regards to C_S. As shown in (2.4), it is the *test-filtered* value of τ_{ij} that is required. If the model coefficient is a function of the three space dimensions, then it is the test-filtered value, $\widehat{C}_S$, that should appear in (2.9) in addition to the grid-level value. For purposes of determining C_S, however, it has been assumed that these coefficients are identical. If the difference between the test-filtered and grid-level values of C_S is large, then (2.9) is at best a rough approximation and may yield erroneous values of the model coefficient.

One method of determining a unique value of C_S from the system of equations (2.9) is by contraction of (2.9) with an appropriate tensor. Germano *et al.* (1991) and Moin *et al.* (1991) used the resolved-scale strain-rate tensor, $\widetilde{S}_{ij}$, to determine C_S in simulations of turbulent channel flow and homogeneous turbulence. This contraction represents an *ad hoc* feature of the dynamic approach. Lilly (1991, private communication) has shown that a least-squares approximation to the solution of (2.9) leads to the following expression for C_S:

$$C_S = \frac{\mathcal{L}^*_{ij}M^*_{ji}}{2M^*_{ij}M^*_{ji}} . \tag{2.11}$$

The model coefficient, C_I, may be obtained directly using (2.8) and the corresponding model for $\mathcal{T}_{kk}$:

$$C_I = \frac{\mathcal{L}_{kk}}{2\widehat{\Delta}^2\widehat{\overline{\rho}}|\widehat{\widetilde{S}}|^2 - 2\widehat{\Delta^2\overline{\rho}|\widetilde{S}|^2}}. \tag{2.12}$$

Consistent with the level of approximation used to model τ_{ij} in (2.5), the subgrid-scale heat flux is approximated using an eddy diffusivity model:

$$q_j = -\overline{\rho}\alpha_T \frac{\partial \widetilde{T}}{\partial x_j}, \tag{2.13}$$

and a turbulent Prandtl number is used to relate α_T to the turbulent eddy viscosity:

$$Pr_T = \frac{\alpha_T}{\nu_T} = \frac{\alpha_T}{C_S\Delta^2|\widetilde{S}|}. \tag{2.14}$$

The procedure to obtain an expression for Pr_T in terms of local flow properties is the same as that used for C_S and C_I. For this case, application of the test filter to the thermal energy equation yields the test-field heat flux, $\mathcal{Q}_j$. This quantity is given by

$$\mathcal{Q}_j = \widehat{\overline{\rho u_j T}} - \frac{\widehat{\overline{\rho u_j}}\,\widehat{\overline{\rho T}}}{\widehat{\overline{\rho}}}, \tag{2.15}$$

and together with q_j is related to the resolved turbulent heat flux, $\mathcal{H}_j$:

$$\mathcal{H}_j = \mathcal{Q}_j - \widehat{q}_j = \widehat{\left(\frac{\overline{\rho u_j}\,\overline{\rho T}}{\overline{\rho}}\right)} - \frac{\widehat{\overline{\rho u_j}}\,\widehat{\overline{\rho T}}}{\widehat{\overline{\rho}}}. \tag{2.16}$$

Equation (2.16) is the counterpart of (2.4) for the thermal energy equation. Assuming that an expression similar to (2.13) may be used to parameterize the heat flux at the test-field level and further that the turbulent Prandtl number is the same at the test and grid levels, then substitution of the models for $\mathcal{Q}_j$ and q_j into (2.16) yields

$$\mathcal{H}_j = \frac{C_S}{Pr_T} R_j, \tag{2.17}$$

where

$$R_j = -\widehat{\overline{\rho}}\widehat{\Delta}^2|\widehat{\widetilde{S}}|\frac{\partial \widehat{\widetilde{T}}}{\partial x_j} + \widehat{\overline{\rho}\Delta^2|\widetilde{S}|\frac{\partial \widetilde{T}}{\partial x_j}}. \tag{2.18}$$

Moin *et al.* (1991) contracted (2.17) with $\partial\widetilde{T}/\partial x_j$ to determine Pr_T. Using the least-squares approach proposed by Lilly, the turbulent Prandtl obtained using (2.17) is

$$\frac{Pr_t}{C_S} = \frac{R_j R_j}{R_j \mathcal{H}_j}. \tag{2.19}$$

The only adjustable parameter of the subgrid-scale models for the turbulent stresses and heat flux shown above is the ratio of filter widths, $\widehat{\Delta}/\Delta$. LES results have been found to be rather insensitive to this ratio (e.g., see Germano *et al.* 1991 and Moin *et al.* 1991). For the results presented in this report, the test-field filter width was twice the grid-level filter width.

Equations (2.11), (2.12), and (2.19) are expressions for the model coefficients which are functions of the three space dimensions and time. In principle, these expressions may be used directly in LES computations. In practice, however, large gradients in the model coefficients, and hence the subgrid stress and heat flux result because of regions in which the denominators of (2.11), (2.12), and (2.19) become small. An additional difficulty which arises is numerical integration of the regions in which the turbulent eddy viscosity is negative. Examination of DNS data of homogeneous turbulence and fully-developed turbulent channel flow by Piomelli *et al.* (1991) has shown that energy transfer in roughly half of the domain is upscale. This in turn implies that the eddy viscosity is negative over a large region of the computational domain. Both the effects of large gradients in the model coefficients as well as negative ν_T have been found to lead to numerical instability in simulations of incompressible and compressible homogeneous turbulence. For this reason, local spatial averages must be applied to the numerators and denominators of (2.11), (2.12), and (2.19). Spatial averaging is required whether C_S and Pr_T are obtained by contraction with $\widetilde{S}_{ij}$ and $\partial\widetilde{T}/\partial x_j$ or M_{ij} and R_j. However, *a priori* tests using DNS data of compressible turbulence have shown that values of C_S and Pr_T obtained by contraction with M_{ij} and R_j exhibit much less scatter than those obtained by contraction with $\widetilde{S}_{ij}$ and $\partial\widetilde{T}/\partial x_j$. Therefore, the model coefficients used in all of the simulations presented in sections 2.2 and 2.3, whether obtained by contraction with $\widetilde{S}_{ij}$ and $\partial\widetilde{T}/\partial x_j$ or M_{ij} and R_j, were obtained by averaging the numerators and denominators of the relevant expressions over the computational box. LES results demonstrating the difference in the two contractions are discussed in section 2.3. Finally, the issue as to whether the nature of the instability in simulations using the dynamic model is strictly numerical or arises because of some underlying physics that the simple eddy-viscosity type models shown above cannot represent remains an area of current research. The reader is referred to the reports by W. Cabot and T. S. Lund in this volume for further discussion of these issues.

2.2 LES of incompressible turbulence

The accuracy of the dynamic model was first tested in LES of decaying, nearly incompressible, isotropic turbulence. A code used by Lee *et al.* (1991) for solution of the compressible Navier-Stokes equations was modified to incorporate the dynamic subgrid-scale model described in section 2.1. For these simulations, LES results were compared to the experimental data of CBC. The initial conditions of the solenoidal velocity field possessed the same radial energy spectrum as in the high Reynolds number experiment of CBC at the first downstream station of the turbulence-generating grid in the wind tunnel ($U_0 t/M = 42$, where $U_0 t$ is the downstream distance, U_0 is the mean velocity, and M is the mesh size). The dilatational

velocity field was initially everywhere zero and remained small throughout the simulations.

The form of C_S and Pr_T in the simulations of nearly incompressible turbulence was not that given by (2.11) and (2.19). For these simulations, the model coefficients were obtained by contraction with $\widetilde{S}_{ij}$ and $\partial\widetilde{T}/\partial x_j$, respectively, i.e.,

$$C_S = \frac{\langle \mathcal{L}^*_{ij} S^*_{ji} \rangle}{2\langle M^*_{ij} S^*_{ji} \rangle}, \tag{2.20}$$

$$\frac{Pr_t}{C_S} = \frac{\langle R_j \frac{\partial \widetilde{T}}{\partial x_j} \rangle}{\langle \mathcal{H}_j \frac{\partial \widetilde{T}}{\partial x_j} \rangle}. \tag{2.21}$$

The angle brackets $\langle\rangle$ denote averaging over the computational box.

Shown in Figure 1 is the temporal development of the resolved scale turbulence kinetic energy for computations using 32^3 and 64^3 grid points. Also shown in this figure is the filtered value of the experimental turbulence energy obtained from CBC. As can be seen from the figure, agreement between the LES results and experimental measurements is excellent for both grid sizes. The computed and experimental radial energy spectra are shown in Figures 2 and 3 for these grid sizes and further demonstrate the good agreement between experimental measurements and LES results obtained using the dynamic model. An estimate of the total turbulence kinetic energy was made using (2.8) to account for subgrid-scale energy. The resolved turbulence energy and the contribution from (2.8) for the subgrid-scale component was within 5% of the experimental values at the two downstream measurement locations from the experiment.

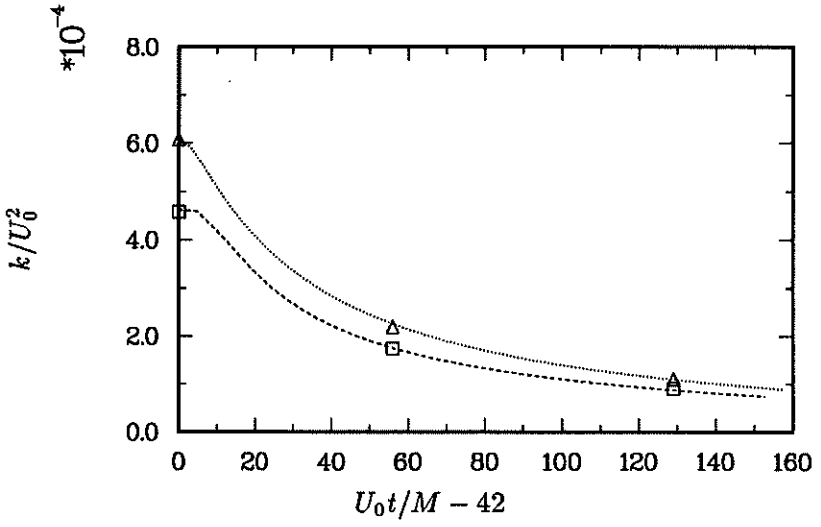

FIGURE 1. Time development of resolved-scale turbulence kinetic energy from LES of isotropic turbulence. □ , filtered data of CBC (32^3); ---- , LES (32^3); △ , filtered data of CBC (64^3); ····· , LES (64^3).

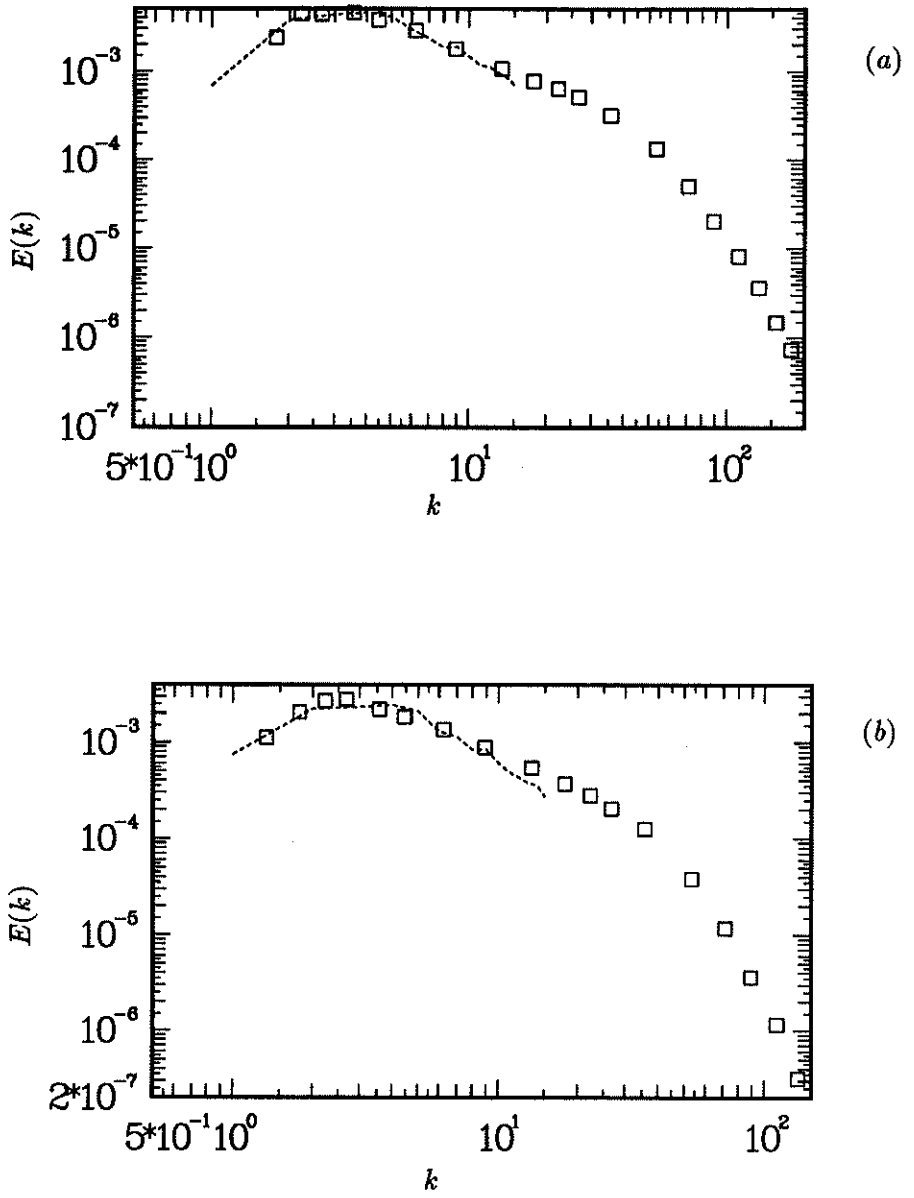

FIGURE 2. Comparison of radial energy spectra to data of CBC. □ , experiment; ---- , LES result (32^3). (*a*) $U_0t/M = 98$. (*b*) $U_0t/M = 171$.

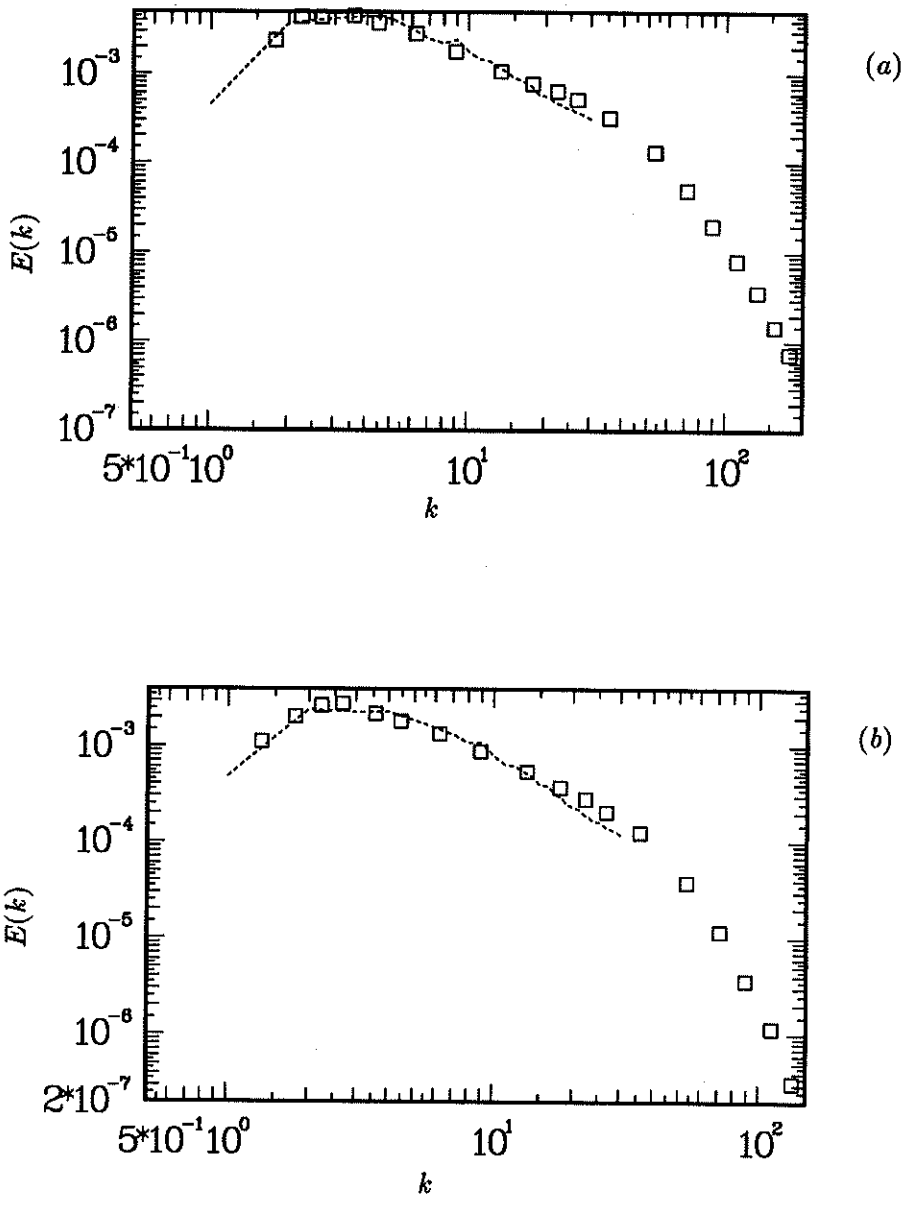

FIGURE 3. Comparison of radial energy spectra to data of CBC. □ , experiment; ---- , LES result (64^3). (*a*) $U_0t/M = 98$. (*b*) $U_0t/M = 171$.

The model coefficients from both the 32^3 and 64^3 LES computations are shown in Figure 4. It may be observed from the figure that the model coefficients attain reasonably stationary values following an initial transient. It is also interesting to note that the equilibrium value of C_S is comparable to the value of the Smagorinsky constant used in early LES studies of isotropic turbulence (e.g., see Mansour *et al.* 1979).

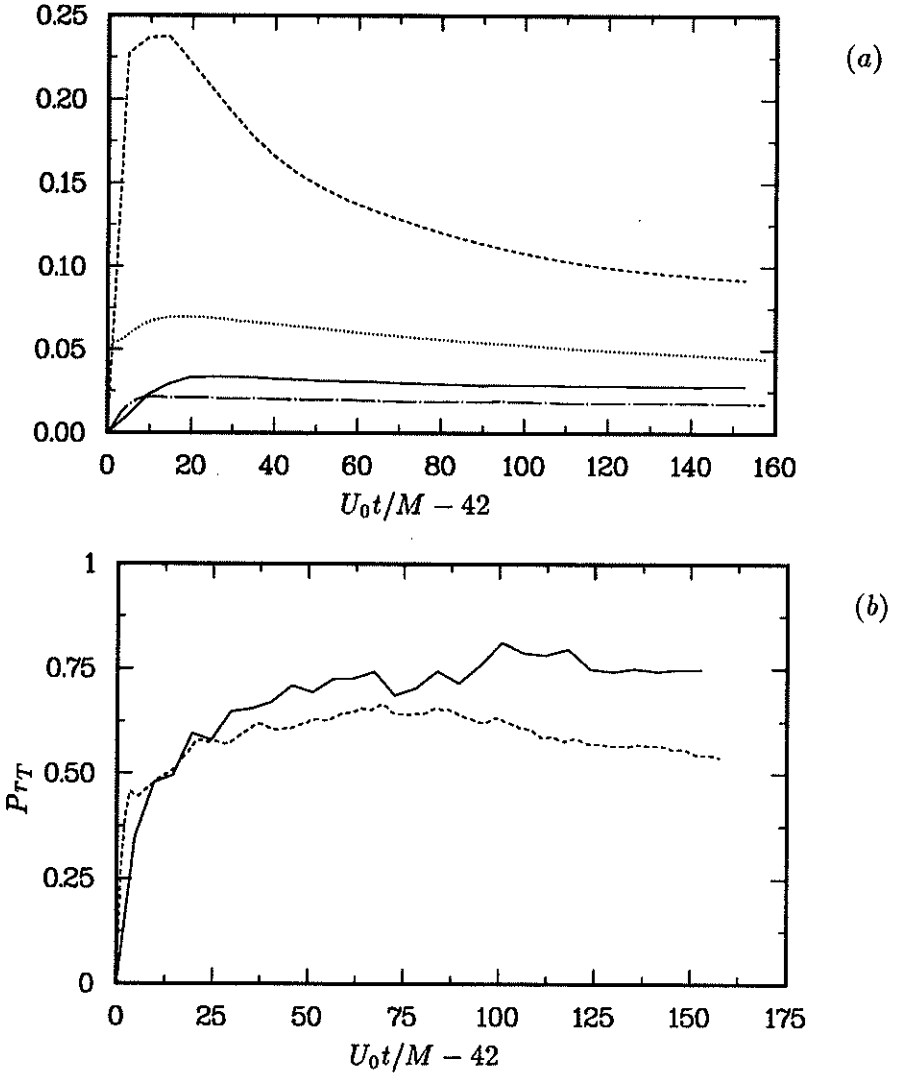

FIGURE 4. (*a*) Time development of model coefficients from LES of isotropic turbulence. ——— , C_S (32^3); ---- , C_I (32^3); —·— , C_S (64^3); ····· , C_I (64^3). (*b*) Time development of turbulent Prandtl number from LES of isotropic turbulence. ——— (32^3); ---- (64^3).

2.3 LES of compressible turbulence

The dynamic model described in section 2.1 was also used in LES of compressible, isotropic turbulence. For these simulations, LES results were compared to filtered DNS data. The DNS results were computed using 96^3 grid points, and the initial energy spectra of the solenoidal and dilatational velocity fields were of the form

$$E(k) \sim k^4 \exp\left[-2(k/k_p)^2\right] . \tag{2.22}$$

The value of k_p, the wavenumber corresponding to the peak in the energy spectrum, was 4 (for a computational box of length 2π per side). The initial velocity fluctuations were scaled such that the fraction of kinetic energy initially residing in the dilatational mode was 20% of the total. The initial density fluctuations were zero, and the initial turbulence Mach number was 0.4. The initial pressure fluctuations were scaled such that the compressible energy was equally partitioned between the kinetic and potential modes. Therefore, these simulations provided a good test of the dynamic model for flows in which the dilatational velocity fluctuations were non-negligible and thermal pressure fluctuations were relatively large. The LES results were computed using 32^3 grid points, and the initial conditions for these computations were identical to the DNS data up to the cutoff wavenumber.

Aside from examining the performance of the dynamic model in LES of fully compressible turbulence, another objective of this phase of the study was examination of the effect of the contraction used to extract the model coefficients on simulation results. LES results obtained using model coefficients extracted using the "least-squares" contraction, i.e., equations (2.11) and (2.19) were compared to results obtained from the "strain-rate" contraction, i.e., equations (2.20) and (2.21). For both the least-squares and strain-rate contractions, the model coefficient C_I was given by equation (2.12). Shown in Figure 5 is the temporal evolution of the model coefficients obtained using both of the contractions. As can be seen from the figure, the value of C_S obtained using the least-squares contraction is 40–50% less than the value obtained from the strain-rate contraction. Figure 5b shows that the turbulent Prandtl number is insensitive to the particular tensor used for the contraction.

Shown in Figure 6 are LES predictions of the resolved scale density fluctuations along with filtered DNS data. As can be seen from the figure, better agreement is obtained between filtered DNS and LES data for the simulation in which the least-squares contraction is used to extract the model coefficients. The decrease in C_S obtained using the least-squares contraction over the strain-rate contraction (see Figure 5a) translates into smaller eddy viscosities and, therefore, less subgrid-scale dissipation. This in turn improves the agreement between filtered DNS density fluctuations and LES results. It is emphasized that the results in Figure 6 are representative of the improvement of LES predictions obtained using the least-squares contraction. For example, LES predictions of energy spectra and temporal development of other thermodynamic quantities are in better agreement with filtered DNS data when using equations (2.11) and (2.19) for C_S and Pr_T, respectively.

Radial energy spectra of the solenoidal and dilatational velocity fields at two instances in the flow evolution are shown in Figures 7a and 7b. The spectra in

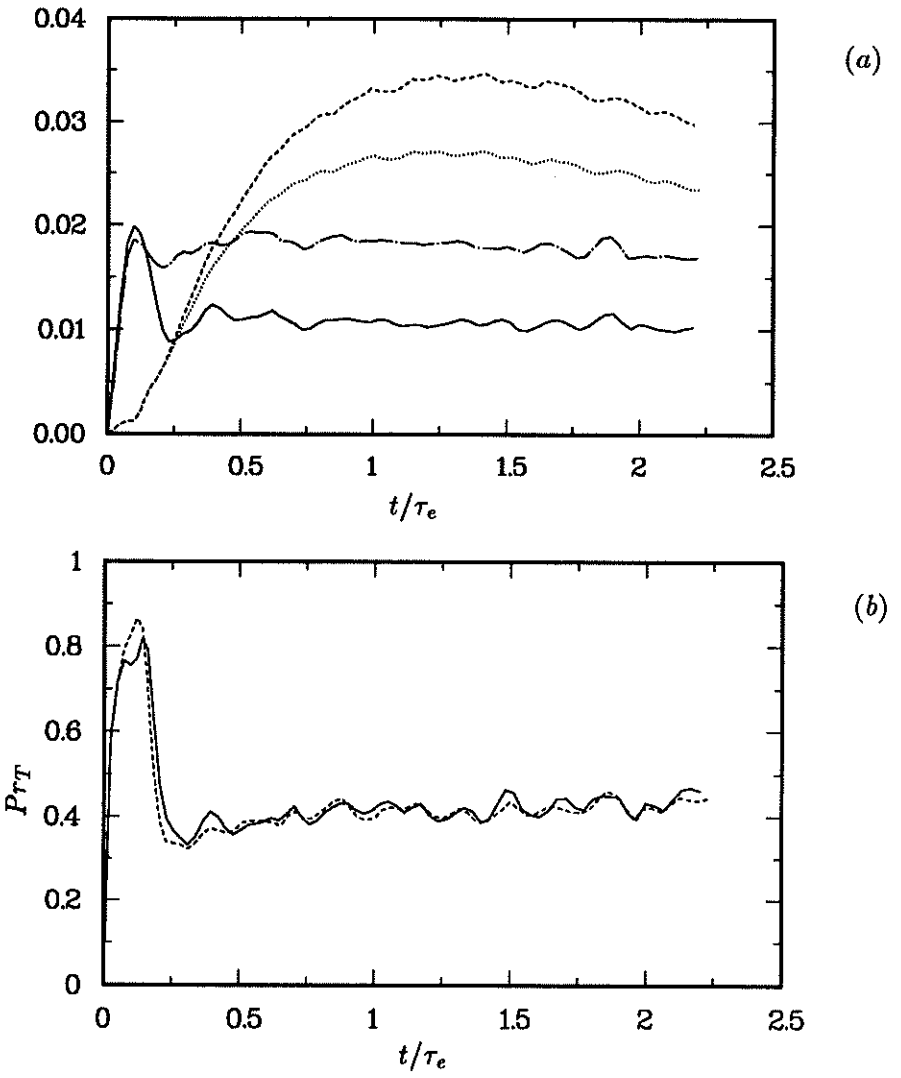

FIGURE 5. (*a*) Time development of model coefficients from LES of isotropic turbulence. ——— , C_S (least-squares); - - - - , C_I (least-squares); —·—, C_S (strain-rate); ····· , C_I (strain-rate). (*b*) Time development of turbulent Prandtl number from LES of isotropic turbulence. ——— (least-squares); - - - - (strain-rate).

Figure 7a corresponds to the time at which the total kinetic energy had decayed 30% from its initial value (0.72 eddy turnover times). From this figure, it is evident that significant subgrid-scale energy resides in the dilatational mode of the velocity field. There is also seen to be very good agreement between the LES and DNS spectra. The spectra in Figure 7b corresponds to the time in the simulation at which the total kinetic energy had decayed 65% from its initial value (1.98 eddy turnover times). This figure also demonstrates the good agreement between LES and DNS spectra. It can be observed from the figure that the evolution of the

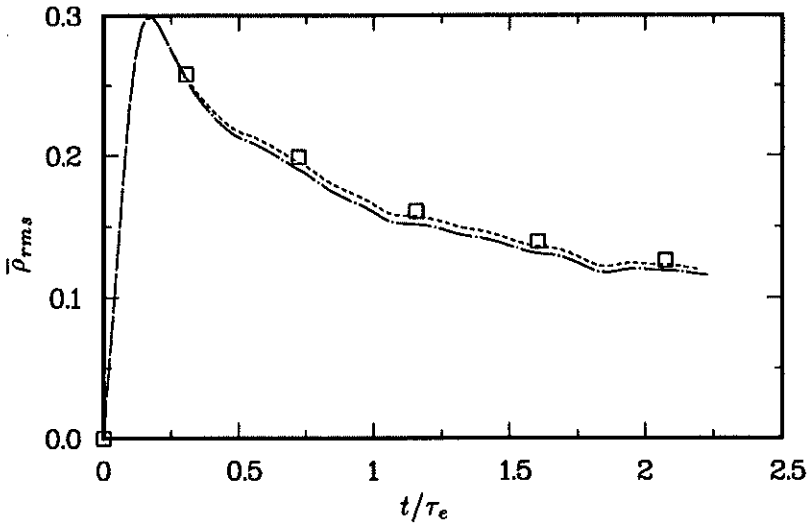

FIGURE 6. Time development of resolved scale density fluctuations from isotropic turbulence. □ , filtered DNS data; ---- , LES (least-squares); —·— , LES (strain-rate).

dilatational velocity field is especially well predicted. At the later time, Figure 7b also shows slightly greater dissipation in the LES spectra of the solenoidal velocity field relative to the DNS spectra.

For all of the results presented thus far, the subgrid-scale energy, q^2, was modeled using Yoshizawa's parameterization (2.8) with the model coefficient given by (2.12). Speziale *et al.* (1988) has shown that the subgrid model formulated by Yoshizawa suffers from the fact that it is valid only for weakly compressible turbulence and a large-scale velocity field which is divergence free. *A priori* tests using of (2.8) by Speziale *et al.* also showed poor correlation between the model expression and exact values of subgrid-scale energy obtained from DNS data of compressible, isotropic turbulence. To test the effect of the model for q^2, an expression derived by Squires & Zeman (1990) which makes explicit account of the effect of large-scale dilatation on subgrid energy was also used in LES computations. The model of Squires & Zeman for q^2 is

$$q^2 = 2\beta\overline{\rho}\Delta^2|\widetilde{S}|^2 + \beta\Delta^2\frac{\nabla\overline{P}\cdot\nabla\widetilde{T}}{\widetilde{T}Pr_T} - \frac{\sqrt{2\beta}}{3}\overline{\rho}\Delta^2|\widetilde{S}|\widetilde{S}_{kk}\,. \tag{2.23}$$

In (2.23) β is the adjustable coefficient which can be determined following the procedure outlined in section 2.1.

LES results obtained using (2.23) for q^2 are compared against those obtained using (2.8) in Figure 8. This figure shows negligible difference in LES results using either expression for q^2. In fact, it can also be observed in Figure 8 that neglect of the subgrid-scale energy, equivalent to setting C_I or β to zero, slightly improves the agreement between LES and DNS results, though this improvement is only of

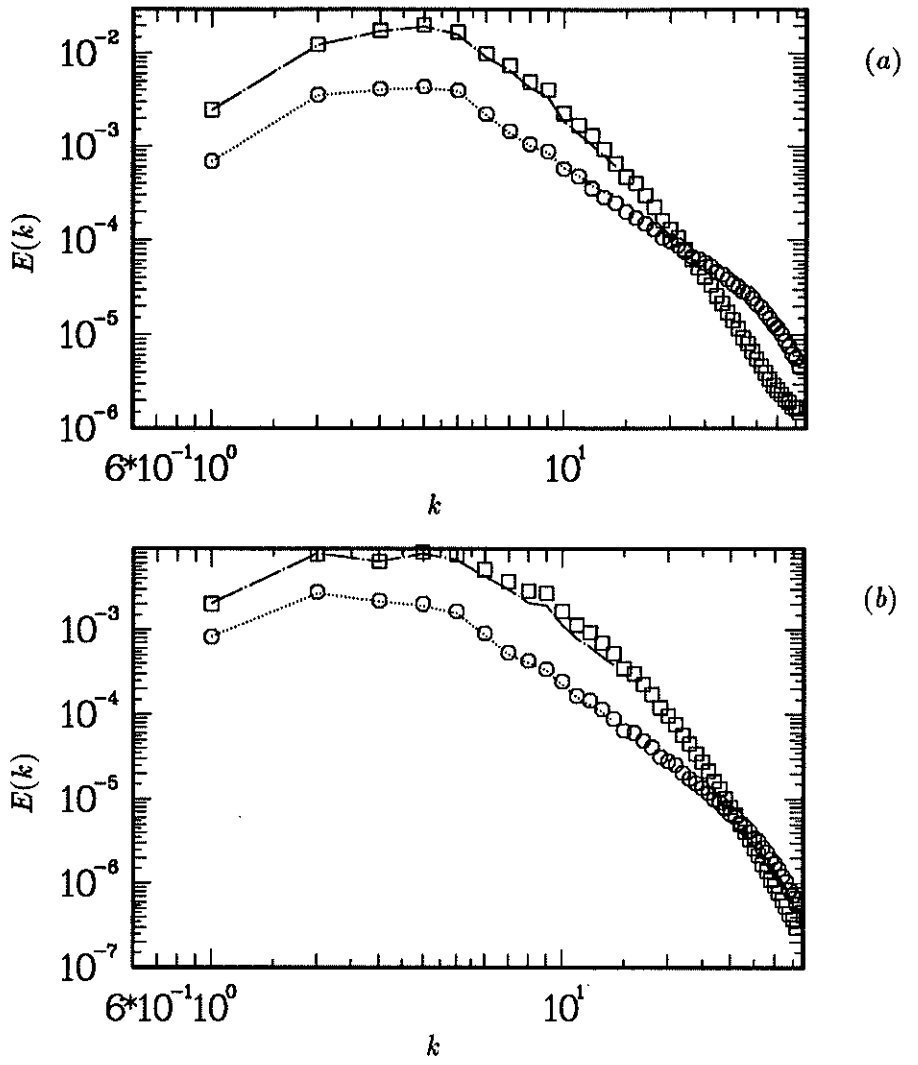

FIGURE 7. Radial energy spectrum from compressible turbulence. (*a*) $t/\tau_e = 0.72$. (*b*) $t/\tau_e = 1.98$. □ , solenoidal velocity (DNS, 96^3); ○ , dilatational velocity (DNS, 96^3); —·— , solenoidal velocity (LES, 32^3); ····· , dilatational velocity (LES, 32^3).

the order of 1%. Erlebacher *et al.* (1990) have proposed a subgrid-scale model in which the effect of subgrid-scale energy is neglected, i.e., $C_I = 0$. Erlebacher *et al.* set $C_I = 0$ based upon the results of *a priori* tests which showed the magnitude of the subgrid-scale energy gradient, $|\nabla q^2|$, was small relative to the magnitude of the pressure gradient, $|\nabla \bar{p}|$. For the simulations of compressible turbulence presented in this section, it was also found that the subgrid-scale energy gradient is small relative to the thermodynamic pressure gradient. Therefore, it is difficult to determine the effect of the model for q^2 on LES results since the contribution of this term in the transport equations is small. In the LES results present in section 2.1, however, the

contribution of the subgrid-scale energy in the transport equations was comparable to (40–50% of) that of the pressure. This was primarily due to the fact that a much larger fraction of the total kinetic energy was contained in the subgrid velocity field. For these cases, it was also found that neglect of q^2 had little influence on LES results. A possible explanation of this may be due to the fact that it is the gradient of subgrid-scale energy which is appears in the momentum equations. Therefore, this term does not affect the overall energy balance of the large-scale field, i.e., it is only the anisotropic part of τ_{ij} which affects the overall transfer of energy from large to small scales.

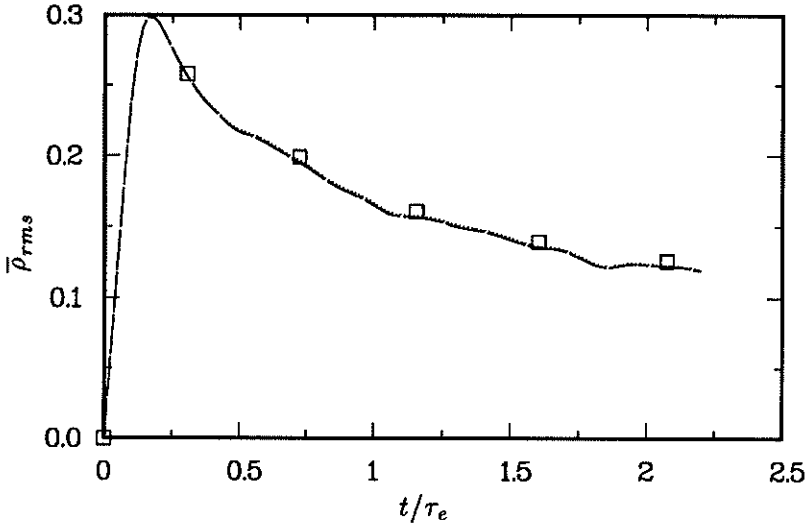

FIGURE 8. Time development of resolved scale density fluctuations from isotropic turbulence. □ , filtered DNS data; ---- , LES, equation (2.12); —·— , LES, equation (2.23); ····· , LES, $C_I = 0$.

3. Future work

The extension of the dynamic modeling concept of Germano *et al.* (1991) has been successfully extended to LES of compressible turbulence. Agreement between LES results and both experimental as well as DNS data is as good or better than previous computations in which model coefficients were calibrated against a specific laboratory or DNS experiment. The model coefficients used in the simulations presented in this report reflect the local temporal properties of the flow field. To take full advantage of the dynamic approach, the model should be applied locally. Initial attempts at using local values of the model coefficients have not yet yielded numerically stable computations. The instability that arises in these computations invariably appears first in the energy equation as two-delta waves in the temperature field. The energy in these waves eventually exhibits exponential growth, resulting in unrealizable values of the temperature.

There are a number of possible causes of the instability in computations using local values of the model coefficients. Numerical difficulties in integration of the

Navier-Stokes equations with highly-variable viscosity as well as deficiencies associated with the Smagorinsky model, or even a combination of both factors, may cause instability.

In the present study, the overall energy transfer from large to small scales was well predicted. However, an aspect not yet addressed for LES of compressible turbulence is incorporation of subgrid dissipation by eddy shocklets. Parameterizations proposed by Squires & Zeman (1990) of shocklet dissipation for subgrid-scale models exhibited very poor correlation between actual and modeled dissipation. It is important that the dynamic model applied in a local sense account for the locally large dissipation due to eddy shocklets.

Logical candidates for subsequent tests of the dynamic model are inhomogeneous flows such as shock-turbulence interaction or shock-boundary layer interaction. For LES computations, shock capturing techniques must first be developed, and this is a complex issue in its own right. Recent work by Yoshizawa (1991) in subgrid-scale model development for compressible turbulence has yielded more sophisticated subgrid-scale models which might be useful for simulation of these more complex flows.

REFERENCES

COMTE-BELLOT, G. & CORRSIN, S. 1971 Simple Eulerian time correlation of full and narrow band velocity signals in grid generated, isotropic turbulence. *J. Fluid Mech.* **48**, 273-337.

ERLEBACHER, G., HUSSAINI, M. Y., SPEZIALE, C. G. & ZANG, T. A. 1990 Toward the large-eddy simulation of compressible turbulent flows. *ICASE Report 90-76.* ICASE, NASA-Langley Research Center.

GERMANO, M. 1990 Averaging invariance of the turbulent equations and similar subgrid-scale modeling. *CTR Manuscript 116.* NASA/Stanford Center for Turbulence Research.

GERMANO, M., PIOMELLI, U., MOIN, P. & CABOT, W. H. 1991 A dynamic subgrid-scale eddy viscosity model. *Phys. Fluids A.* **3**, 1760-1765.

LEE, S., MOIN, P. & LELE, S. K. 1991 Eddy shocklets in decaying compressible turbulence. *Phys. Fluids A.* **3**, 657-664.

MANSOUR, N. N., MOIN, P., FERZIGER, J. H. & REYNOLDS, W. C. 1979 Improved methods for large eddy simulations of turbulence *Turbulent Shear Flows I.* Springer-Verlag (Berlin), pp. 386-401.

MOIN, P., SQUIRES, K., CABOT, W. & LEE, S. 1991 A dynamic subgrid-scale model for compressible turbulence and scalar transport. *Phys. Fluids A.* **3**, 2746-2757.

PIOMELLI, U., CABOT, W. H., MOIN, P. & LEE, S. 1991 Subgrid-scale backscatter in transitional and turbulent flows. *Phys. Fluids A.* **3**, 1766.

SMAGORINSKY, J. 1963 General circulation experiments with the primitive equations. I. The basic experiment. *Mon. Weather Rev..* **91**, 99-164.

SPEZIALE, C. G., ERLEBACHER, G., ZANG, T. A. & HUSSAINI, M. Y. 1988 The subgrid-scale modeling of compressible turbulence. *Phys. Fluids A.* **31,** 940-942.

SQUIRES, K. D. & ZEMAN, O. 1990 On the subgrid-scale modeling of compressible turbulence. *Proceedings of the 1990 Summer Program.* NASA/Stanford Center for Turbulence Research, pp. 47-59.

YOSHIZAWA, A. 1986 Statistical theory for compressible turbulent shear flows, with application to subgrid modeling. *Phys. Fluids A.* **29,** 2152-2164.

YOSHIZAWA, A. 1991 Subgrid-scale modeling of compressible turbulent flows. *Phys. Fluids A.* **3,** 714-716.